Volume 8
Number 22
14 June 2020
Pages 4703–4964

Journal of Materials Chemistry B

Materials for biology and medicine

rsc.li/materials-b

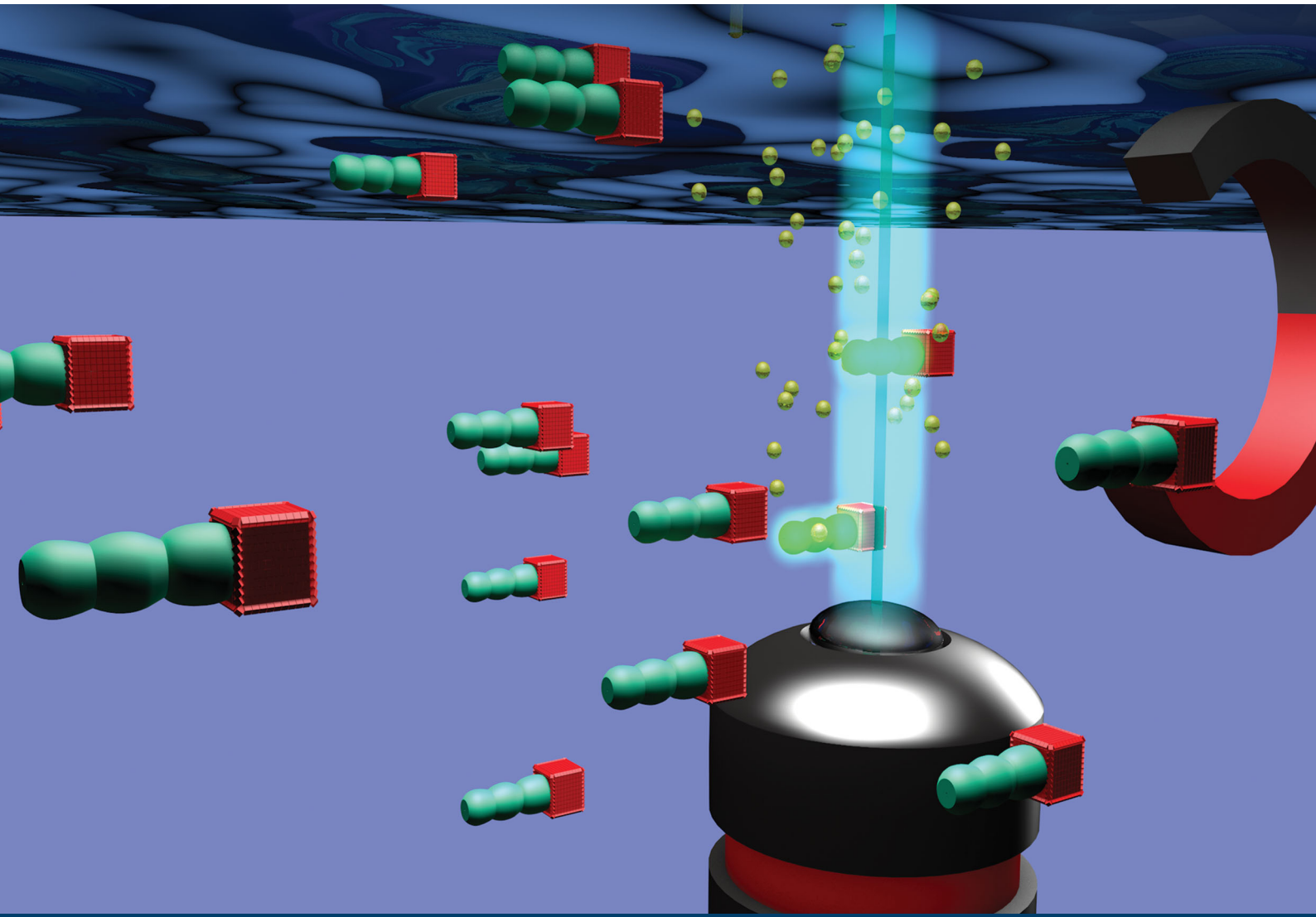

Themed issue: Hybrid Nanoparticle Composites

ISSN 2050-750X

ROYAL SOCIETY OF CHEMISTRY

COMMUNICATION

Helmut Cölfen, Juan-Manuel García-Ruiz *et al.*
Light-switchable anchors on magnetized biomorphic microcarriers

Journal of Materials Chemistry B

ROYAL SOCIETY OF CHEMISTRY

COMMUNICATION

View Article Online
View Journal | View Issue

Check for updates

Cite this: *J. Mater. Chem. B*, 2020, **8**, 4831

Received 29th December 2019,
Accepted 24th April 2020

DOI: 10.1039/c9tb02955a

rsc.li/materials-b

Light-switchable anchors on magnetized biomorphic microcarriers

Julian Opel,†[ab] Lisa-Catherine Rosenbaum,†[c] Julian Brunner,[a] Anne Staiger,[ac] Ramon Zimmermanns,[a] Matthias Kellermeier,[d] Tanja Gaich,[c] Helmut Cölfen*[a] and Juan-Manuel García-Ruiz*[b]

Microcarriers with the ability to release and catch substances are highly desired metamaterials and difficult to obtain. Herein, we report a straightforward strategy to synthesize these materials by combining silica-biomorphs with mesocrystals. An easy access to microcarrier hulls with covalently bound spiropyrans as light-switchable anchor points is presented.

Introduction

The so-called silica-biomorphs are purely inorganic composite materials that exhibit outstanding shapes.[1–3] They are prepared in alkaline, silica-rich solutions containing earth-alkaline metal ions, such as Ba^{2+}, Sr^{2+} and Ca^{2+}.[4,5] Their formation mechanism is assumed to be based on autocatalytic co-precipitation of earth-alkaline carbonates and silica linked to a local pH cycling induced by alternating silica and carbonate precipitation.[6–8] A huge variety of self-assembled carbonate nanorods are attractive for several applications. The elongated architecture of worm-like and helicoidal shaped biomorphs renders them with the potential to be used as microcarrier hulls.[9] Magnetic nanoparticles like magnetite nanocubes are used as responding units, which are needed for controlled movement through various media.[10,11] The benefit of this system is the ability to attach mesocrystals at specific sides of the biomorph (*cf.* Fig. 1).[9,12] Mesocrystals form in a non-classical pathway *via* the oriented assembly of non-spherical nanocrystals into superlattices.[13,14]

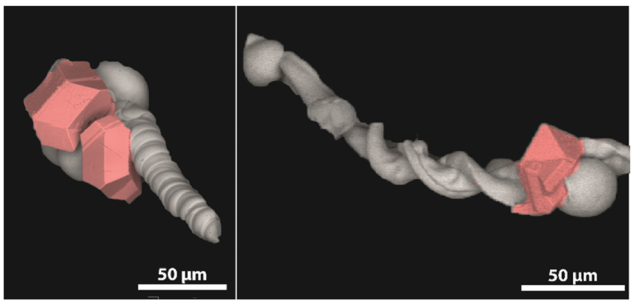

Fig. 1 Scanning electron micrographs of a biomorph worm (left) and a biomorph helix (right) decorated with magnetite mesocrystals (highlighted in red) at the globular apex of the structures.

In order to create further functionality, the structures must be equipped with an additional responding unit that allows addressing of a switchable anchor point for controlled compound load/release. Previous studies employed post-functionalization by the use of silane coupling chemistry.[9,15]

The incorporation of light-switchable molecules into various systems and the development of so-called dynamic materials came into the focus of attention during the last decades. Not only the synthesis of materials for data storage,[16] electronic devices[17] or sensors[18] but also the biological applications of photo-responsive compounds, *e.g.* in photopharmacology,[19–21] have been investigated. Photo-switchable molecules show reversible transformation between at least two different thermodynamically stable isomers induced by irradiation with light of a particular wavelength. Among the wide range of photo-switches, spiropyrans achieved a privileged status since they enable the production of materials that are responsive to multiple external stimuli in an orthogonal fashion. The two isomeric structures of a spiropyran show vastly different properties, which results in an isomerization process that is not only induced by irradiation with light but also by several other external stimuli including temperature, solvent and pH-value.[22] In addition, the covalent

[a] *Physical Chemistry, University of Konstanz, Universitätsstrasse 10, D-78457 Konstanz, Germany. E-mail: helmut.coelfen@uni-konstanz.de; Fax: +49 7531 88 3139; Tel: +49 7531 88 4063*
[b] *Laboratorio de Estudios Cristalográficos, Instituto Andaluz de Ciencias de la Tierra (CSIC-UGR), Avenida de las Palmeras No. 4, E-18100 Armilla, Granada, Spain. E-mail: juanmanuel.garcia@csic.es; Fax: +34 958 552620; Tel: +34 958 230000*
[c] *Organic Chemistry, University of Konstanz, Universitätsstrasse 10, D-78457 Konstanz, Germany. E-mail: Tanja.Gaich@uni-konstanz.de*
[d] *Material Physics, BASF SE, GMC/O – G201, Carl-Bosch-Strasse 38, D-67056 Ludwigshafen, Germany. E-mail: matthias.kellermeier@basf.com; Fax: +49 621 66 43388; Tel: +49 621 60 43388*
† JO and LCR wrote the paper and have contributed equally to the work.

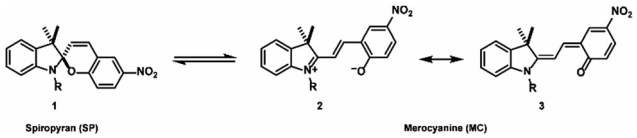

Fig. 2 Typical structural formula of a spiroindolinopyran.

attachment of spiropyran units to a solid support results in numerous advantages compared to the non-immobilized counterparts, including an improved fatigue resistance,[23,24] and the possibility to obtain biocompatible photoresponsive materials.[25,26]

The incorporation of silane-containing switchable molecules like spiropyrans is a desired method to obtain new metamaterials.[22,27]

The typical structural formula of a spiroindolinopyran (SP) is shown in Fig. 2, consisting of an indoline and a chromene moiety, which are connected *via* a spiro-center. The isomeric merocyanine (MC) is accessible by heterolytic cleavage of the C_{spiro}–O bond induced by irradiation with UV-light. The population of the excited state is followed by an intersystem crossing process to the corresponding triplet state in which the ring opening takes place.[28] Internal rotation in the ground state to the *cis*- and *trans*-isomers is in most cases followed by a thermal isomerization to the *trans*-isomer. The open-ring isomer exists as either zwitterionic (**2**) or quinoidal species (**3**).

Merocyanine often shows strong fluorescence and exhibits a remarkably higher affinity to different chemical structures,[29] a property that is caused by the additional free oxygen acting as a donor function. The zwitterionic merocyanine has already been described as a ligand for (divalent) metal ions[30–32] whereas the neutral spiropyran is a rather unfavorable donor. Utilizing the huge differences in the properties of the isomers, multi-fluorescent hybrid particles,[33] traps for ions[34] and small molecules[35] are prepared, the hydrophobicity of solid surfaces[36] can be tuned reversibly, and the electrochemical properties of a surface[37] are controlled. Reverse isomerization to the initial spiro-compound is possible by either thermal relaxation or irradiation with visible light. These properties made the spiropyran–merocyanine system to be the focus of our interest with regard to the design of a magnetized biomorphic microcarrier system.

Experimental

Materials and methods

The purchased ethyl acetate and hexane for column chromatography were of technical grade and distilled before usage. All other chemicals were purchased from Sigma-Aldrich and TCI and used without further purification. NMR spectra were recorded on a Bruker Avance III 400. Chemical shifts are referred relative to the solvent residual peaks. Data are reported as: chemical shift, multiplicity, coupling constant *J*, and integration. Infrared spectra (IR) of thin films were recorded on a PerkinElmer Spectrum 100 spectrometer with an ATR-unit. UV/Vis spectra were recorded on a Cary 50 spectrometer. High-resolution mass spectra (HRMS) were recorded on a Fischer Scientific Orbitrap Velos Pro. Scanning electron micrographs (SEM) were recorded on a Hitachi table-top SEM TM3000 with an acceleration voltage of 15 kV. Laser scanning micrographs (LSM) were recorded on a Zeiss LSM 700 with a 63×/1.40 Plan Apochromat (Oil) objective and with laser diodes (405, 488, 555 and 637 nm). The images were recorded in fluorescence and transmission channel on two photomultipliers.

Synthesis of magnetite mesocrystal silica-biomorph composites

The formation of silica biomorphs and the needed functionalization for mesocrystal attachment is described elsewhere.[9] The analysis of the structures was performed by IR-spectroscopy, light- and scanning electron microscopy.

Synthesis of compound 6

Compound **6** was synthesized in two steps from commercially available 2,3,3-trimethylindolenine by a literature-known procedure.[38] The obtained spectroscopic data are consistent with those reported previously.

^{1}H-NMR (400 MHz, DMSO): δ [ppm] = 12.24 (bs, 1H), 8.24 (d, $^3J_{HH}$ = 2.8 Hz, 1H), 8.03 (dd, $^3J_{HH}$ = 2.8′, 9.0 Hz, 1H), 7.24 (d, $^3J_{HH}$ = 10.3 Hz, 1H), 7.17–7.13 (m, 2H), 6.88 (d, $^3J_{HH}$ = 9.0 Hz, 1H), 6.83 (t, $^3J_{HH}$ = 7.5 Hz, 1H), 6.69 (d, $^3J_{HH}$ = 7.8 Hz, 1H), 6.03 (d, $^3J_{HH}$ = 10.3 Hz, 1H), 3.57–3.39 (m, 2H), 2.64–2.44 (m, 2H), 1.21 (s, 3H), 1.10 (s, 3H).

Synthesis of compound 7

Compound **6** (2.30 g, 6.05 mmol, 1.0 eq.), EDC·HCl (1.28 g, 6.66 mmol, 1.1 eq.) and DMAP (0.74 g, 6.05 mmol, 1.0 eq.) were dissolved in CH_2Cl_2 (20 mL) and stirred for 10 minutes. (3-Aminopropyl)triethoxysilane (1.41 g, 6.35 mmol, 1.05 eq.) was added dropwise and the reaction was stirred for 20 hours at room temperature. The solvent was removed under reduced pressure and the crude product was purified by flash chromatography on silica gel (2 : 1 ethyl acetate/hexane). Compound **7** was obtained as a red solid (2.71 g, 4.64 mmol, 77% yield).

^{1}H-NMR (400 MHz, DMSO): δ [ppm] = 8.20 (d, $^3J_{HH}$ = 2.8 Hz, 1H), 7.99 (dd, $^3J_{HH}$ = 2.8, 8.9 Hz, 1H), 7.86 (t, $^3J_{HH}$ = 5.5 Hz, 1H), 7.18 (d, $^3J_{HH}$ = 10.4 Hz, 1H), 7.14–7.09 (m, 2H), 6.85 (d, $^3J_{HH}$ = 9.0 Hz, 1H), 6.78 (dt, $^3J_{HH}$ = 7.4, 0.6 Hz, 1H), 6.65 (d, $^3J_{HH}$ = 7.7 Hz, 1H), 5.97 (d, $^3J_{HH}$ = 10.4 Hz, 1H), 3.70 (q, $^3J_{HH}$ = 7.0Hz, 6H), 3.49–3.29 (m, 2H), 3.01–2.87 (m, 2H), 2.43–2.27 (m, 2H), 1.41–1.33 (m, 2H), 1.18 (s, 3H), 1.12 (t, $^3J_{HH}$ = 7.0 Hz, 9H), 1.07 (s, 3H), 0.49–0.45 (m, 2H).

^{13}C-NMR (101 MHz, DMSO): δ [ppm] = 170.1, 159.2, 146.4, 140.5, 135.6, 127.9, 127.5, 125.6, 122.7, 121.9, 121.6, 119.1, 118.9, 115.4, 106.7, 106.6, 57.6, 52.4, 41.3, 39.5, 34.9, 25.5, 22.7, 19.4, 18.2, 7.4.

IR (ATR): $\tilde{\nu}$ [cm^{-1}] = 3307, 2973, 2928, 1740, 1639, 1611, 1511, 1479, 1334, 1273, 1075, 951, 919, 808, 787, 748.

HRMS: *m*/*z* calculated for $C_{30}H_{42}N_3O_7Si^+$: 584.2787; found: 584.2785.

Functionalization of mesocrystal-biomorph composites with compound 7

A 1% solution of compound **7** in a mixture of EtOH:water (95 : 5) was prepared. 10 mg of mesocrystal biomorph composites were

incubated in 2 mL of the solution overnight. After reaction, the material was centrifuged and washed several times with milliQ water. The structures were dried in a vacuum oven at 40 °C and reduced pressure.

Results and discussion

The synthesis of a silane-functionalized spiropyran is desired for a carrier system based on mesocrystal-biomorph composites (MCBCs). Spiropyrans for the desired silica-modification were already published in the literature,[27] but their accessibility and feasibility were improved in this approach. Based on a literature-known synthesis of a spiropyran bearing a carboxylic acid group,[39] the desired compound was accessible by peptide coupling with 3-aminopropyl triethoxysilane. The reaction scheme is shown in Fig. 3A. Compound 7 was subsequently immobilized on silica-biomorphs. The attachment of functional silanes to various biomorphs was already proven and allowed the desired functionalization of the particle surface with spiropyrans.[15] The scheme of this procedure is shown in Fig. 3B.

Silica-biomorphs were precipitated from barium-containing alkaline silica sol through continued CO_2 diffusion into the sol. The structures remained in the mother sol for 16 h to reach the secondary precipitation stage, where an outer silica shell and additional witherite attach to the structures.[9] A thicker silica layer around the structures is desirable to improve the stability once the inner core dissolves for an improved carrier capacity of the MCBCs. Selective secondary precipitation of witherite crystals around the tips of the structures is desired to induce the heterogeneous magnetite mesocrystal formation. The obtained solid from the biomorph synthesis was rinsed several times with deionized water and dried. The biomorph powder mainly consisted of worm-like braids and helicoidal structures, decorated with witherite crystals on the former globular tips of the biomorphs. The structures were transferred into a magnetite nanocube solution in THF containing a certain amount of oleic acid. The biomorphs act as substrates for the mesocrystal formation. Mesocrystals were formed through gas phase diffusion of the anti-solvent (ethanol) into the magnetite nanocube solution. The particle and the oleic acid concentrations were accurately chosen in order to generate mesocrystals in the range of the tip size (*cf.* Fig. 1). The decreased nanocube concentration leads to smaller mesocrystals and a lower total magnetite loading of the structures. The result is a different responding behaviour in the magnetic field. The decreased oleic acid concentration results in an increased number of smaller mesocrystals. The total magnetite loading remained constant.[9] The obtained MCBCs allow a further post-functionalization treatment with synthesized compound 7 by incubation of the structures in a 1 wt% solution in ethanol/water (95 : 5) for several hours. The generated

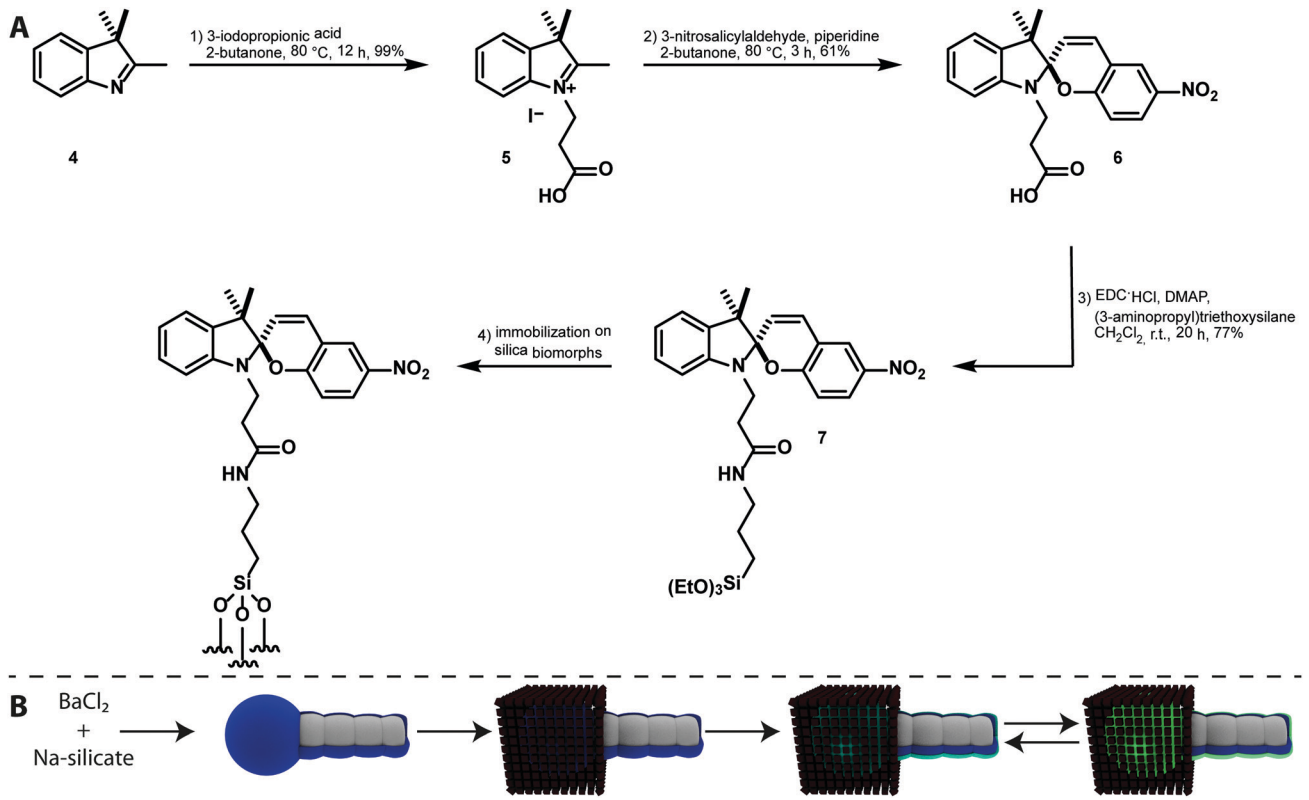

Fig. 3 (A) Synthesis route of the silane functionalized spiropyran (target compound **7**). (B) Formation scheme of the light switchable MCBCs *via* the selective formation of magnetite mesocrystals around silica-biomorphs tips and the post functionalization of their silica shell with compound **7** and its ability of light induced switching on the MCBC surface which induces the glowing (bright green).

functionalized silica layer can be seen in Fig. 3B as a blue layer in the SP form. The UV-irradiation of the material induces the spiro-compound to switch to the MC form, which is indicated by the glowing green colored layer (Fig. 3B). As previously mentioned in the literature, the vastly different properties of the two isomers can be further used for selective catch and release of compounds.[27]

To prove the postulated scheme of the formation of light switchable MCBCs, laser scanning microscopy (LSM) was used. A selective switching of the SP by using the bleach mode was induced with a different wavelength. Therefore, the excitation and emission spectra of compound **7** were recorded and are shown in Fig. 4A. The black spectrum shows the excitation spectrum of the SP-form detecting the intensity of fluorescence at 625 nm while the excitation wavelength changes. The spectrum has a maximum at 555 nm and a shoulder at 520 nm. In addition, several emission spectra were recorded to elaborate the obtained fluorescence as the subject of the excitation wavelength. Using an excitation wavelength of 555 nm, the highest fluorescence intensity was obtained (green spectrum), while an excitation wavelength of 490 nm exhibited lower fluorescence yields (blue spectrum). Nevertheless, the excitation wavelength of 490 nm is the most important result due to the equipped analysing lasers on the LSM. For the fluorescence experiments on the LSM, the imaging was performed with a 488 nm laser (1% laser power, pin hole: 1 a.u.). Imaging the structures with visible light continuously decreased the obtained fluorescence. The degradation of fluorescence is worse with the 555 nm laser, which was additionally chosen in other experiments to turn off the fluorescence while switching the MC back to the SP form. To generate a high amount of fluorescent MCs on the surface, the structures were "bleached" in a region of interest (ROI) with a 405 nm laser (20% laser power, 4 scans). The result is shown in Fig. 4B. The bleaching of the ROI occurred after the first and every third following cycle, indicated by the bluish bars. The measured data originated from a programmed times series. A continuous decrease of the fluorescence intensity in the 3 steps after excitation to a level lower than before the bleaching explains the ongoing decrease of the overall fluorescence intensity. The effect becomes even clearer by considering several cycles. An example is shown in Fig. 4C, where 72 cycles are recorded in the same area. To visualize this effect, Fig. 4D shows a functionalized MCBC in its OFF state, before the frame was illuminated with 405 nm light. Fig. 4E shows the activated structure after excitation. It has to be mentioned that the pictures show a lower end of a functionalized biomorph worm, and the lowest part is in focus. The pin hole cuts off the fluorescent light emitted from the upper part, allowing for an improved image quality and spatial resolution. Therefore, LSM seems to be an appropriate method to prove the incorporation of the functional silane on the structures. This has also been shown in previous studies[15] and demonstrates the suitability of spiropyrans as switchable anchor points on biomorph-based microcarriers.

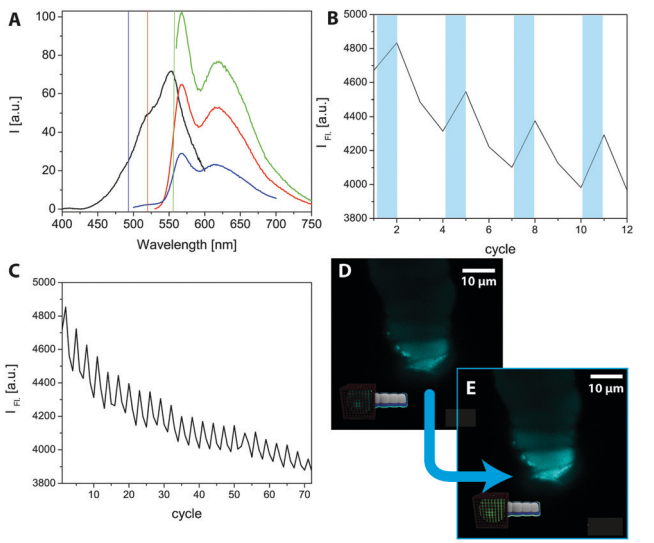

Fig. 4 (A) Excitation (black) and emission spectra of the synthesized compound **7** in ethanol. The vertical coloured lines correspond to the excitation wavelength (blue: 490 nm; red: 520 nm; green: 555 nm). (B) ROI (region of interest) intensity measurement over twelve scanning cycles on the LSM. Bleaching of the region (405 nm; 20% laser power; 4 scans; after the 1st and every following 3rd image) is indicated as bluish areas. (C) Long-term cycling at the ROI over 72 cycles with the same settings chosen for B. (D) LSM image (excitation wavelength: 488 nm, 1% laser power) in false colours of a SP functionalized structure in the OFF (SP) state. (E) LSM image of a SP functionalized structure in the ON (MC) state.

Conclusions

This work highlights a rationally designed pathway to generate easily accessible microcarriers by utilising the silane chemistry toolbox linked to light switchable spiropyrans and the exceptionally shaped ultrastructures called silica-biomorphs. On top a magnetite mesocrystal is used as a responding unit, which results in a full functional metamaterial extending the frontiers in all three used fields (biomorphs, mesocrystals and spiropyrans). The materials described here have potential in a number of applications. Since it is already known from the literature that the merocyanine form can bind metal cations,[30–32] the microcarriers could be used for the transport of metal ions by a magnetic field. Ion release by switching to the spiropyran form would allow reactions of the released cations like catalysis, mineralization, complexation, *etc.* One could also think of binding polar nanoparticles to the merocyanine form, which can be released by light at the location of interest. Also, polar drugs could be bound, transported and released. If the spiropyran form could be used for binding of unipolar species (drugs, molecules, *etc.*), release by light switching to the merocyanine form would enhance the application spectrum of the microcarriers a lot. Future studies will show exciting applications, which will become possible with the mesocrystal functionalized biomorph microcarriers.

Authors contributions

JO and HC conceived the project. LCR and AS synthesized and analysed compound **7** under supervision of TG. JO, JB and RZ

designed the magnetized biomorphs. JO and AS functionalized the biomorphs with compound 7. JO, AS and RZ performed the microscope experiments. The results were discussed by all authors.

Conflicts of interest

The authors declare that there is no conflict of interests regarding the publication of this communication.

Acknowledgements

The authors thank the bioimaging center Konstanz for providing the LSM700 and the European Research Council under the European Unions's Seventh Framework Programme (FP7/2007–2013)/ERC grant agreement no. 340863. The Deutsche Forschungsgemeinschaft (DFG) is acknowledged for funding of the work on mesocrystals within SFB 1214 (project B1).

Notes and references

1 J. M. Garcia-Ruiz, S. T. Hyde, A. M. Carnerup, A. G. Christy, M. J. Van Kranendonk and N. J. Welham, *Science*, 2003, **302**, 1194–1197.
2 J. M. García-Ruiz, E. Melero-García and S. T. Hyde, *Science*, 2009, **323**, 362–365.
3 M. Kellermeier, H. Colfen and J. M. Garcia-Ruiz, *Eur. J. Inorg. Chem.*, 2012, 5123–5144.
4 E. Nakouzi and O. Steinbock, *Sci. Adv.*, 2016, **2**, e1601144.
5 E. Nakouzi, R. Rendina, G. Palui and O. Steinbock, *J. Cryst. Growth*, 2016, **452**, 166–171.
6 M. Montalti, G. Zhang, D. Genovese, J. Morales, M. Kellermeier and J. M. García-Ruiz, *Nat. Commun.*, 2017, **8**, 14427.
7 J. Opel, M. Hecht, K. Rurack, J. Eiblmeier, W. Kunz, H. Colfen and M. Kellermeier, *Nanoscale*, 2015, **7**, 17434–17440.
8 M. Kellermeier, E. Melero-García, W. Kunz and J. M. García-Ruiz, *J. Colloid Interface Sci.*, 2012, **380**, 1–7.
9 J. Opel, J. Brunner, R. Zimmermanns, T. Steegmans, E. Sturm, M. Kellermeier, H. Cölfen and J. M. García-Ruiz, *Adv. Funct. Mater.*, 2019, **0**, 1902047.
10 M. V. Kovalenko, M. I. Bodnarchuk, R. T. Lechner, G. Hesser, F. Schäffler and W. Heiss, *J. Am. Chem. Soc.*, 2007, **129**, 6352–6353.
11 S. Disch, E. Wetterskog, R. P. Hermann, G. Salazar-Alvarez, P. Busch, T. Brückel, L. Bergström and S. Kamali, *Nano Lett.*, 2011, **11**, 1651–1656.
12 J. Brunner, I. A. Baburin, S. Sturm, K. Kvashnina, A. Rossberg, T. Pietsch, S. Andreev, E. Sturm and H. Cölfen, *Adv. Mater. Interfaces*, 2017, **4**, 1600431.
13 H. Cöelfen and M. Antonietti, *Mesocrystals and nonclassical crystallization*, John Wiley & Sons, 2008.
14 H. Cölfen and M. Antonietti, *Angew. Chem., Int. Ed.*, 2005, **44**, 5576–5591.
15 J. Opel, F. P. Wimmer, M. Kellermeier and H. Cölfen, *Nanoscale Horiz.*, 2016, **1**, 144–149.
16 M. H. Sharifian, A. R. Mahdavian and H. Salehi-Mobarakeh, *Langmuir*, 2017, **33**, 8023–8031.
17 D. Kim, H. Jeong, H. Lee, W.-T. Hwang, J. Wolf, E. Scheer, T. Huhn, H. Jeong and T. Lee, *Adv. Mater*, 2014, **26**, 3968–3973.
18 S. Heng, P. Reineck, A. K. Vidanapathirana, B. J. Pullen, D. W. Drumm, L. J. Ritter, N. Schwarz, C. S. Bonder, P. J. Psaltis, J. G. Thompson, B. C. Gibson, S. J. Nicholls and A. D. Abell, *ACS Omega*, 2017, **2**, 6201–6210.
19 W. A. Velema, W. Szymanski and B. L. Feringa, *J. Am. Chem. Soc.*, 2014, **136**, 2178–2191.
20 W. Szymański, J. M. Beierle, H. A. V. Kistemaker, W. A. Velema and B. L. Feringa, *Chem. Rev.*, 2013, **113**, 6114–6178.
21 M. Borowiak, W. Nahaboo, M. Reynders, K. Nekolla, P. Jalinot, J. Hasserodt, M. Rehberg, M. Delattre, S. Zahler, A. Vollmar, D. Trauner and O. Thorn-Seshold, *Cell*, 2015, **162**, 403–411.
22 R. Klajn, *Chem. Soc. Rev.*, 2014, **43**, 148–184.
23 J. Whelan, J. T. C. Wojtyk and E. Buncel, *Chem. Mater.*, 2008, **20**, 3797–3799.
24 A. Radu, R. Byrne, N. Alhashimy, M. Fusaro, S. Scarmagnani and D. Diamond, *J. Photochem. Photobiol., A*, 2009, **206**, 109–115.
25 M.-Q. Zhu, G.-F. Zhang, C. Li, M. P. Aldred, E. Chang, R. A. Drezek and A. D. Q. Li, *J. Am. Chem. Soc.*, 2011, **133**, 365–372.
26 Y.-H. Chan, M. E. Gallina, X. Zhang, I. C. Wu, Y. Jin, W. Sun and D. T. Chiu, *Anal. Chem.*, 2012, **84**, 9431–9438.
27 E. Aznar, R. Casasús, B. García-Acosta, M. D. Marcos, R. Martínez-Máñez, F. Sancenón, J. Soto and P. Amorós, *Adv. Mater.*, 2007, **19**, 2228–2231.
28 H. Gorner, *Phys. Chem. Chem. Phys.*, 2001, **3**, 416–423.
29 N. Shao, J. Y. Jin, S. M. Cheung, R. H. Yang, W. H. Chan and T. Mo, *Angew. Chem., Int. Ed.*, 2006, **45**, 4944–4948.
30 K. H. Fries, J. D. Driskell, G. R. Sheppard and J. Locklin, *Langmuir*, 2011, **27**, 12253–12260.
31 M. Inouye, K. Akamatsu and H. Nakazumi, *J. Am. Chem. Soc.*, 1997, **119**, 9160–9165.
32 T. Suzuki, T. Kato and H. Shinozaki, *Chem. Commun.*, 2004, 2036–2037, DOI: 10.1039/B407342H.
33 T. Wu, G. Zou, J. Hu and S. Liu, *Chem. Mater.*, 2009, **21**, 3788–3798.
34 K. Fries, S. Samanta, S. Orski and J. Locklin, *Chem. Commun.*, 2008, 6288–6290, DOI: 10.1039/B818042C.
35 E. Aznar, R. Casasús, B. García-Acosta, M. D. Marcos, R. Martínez-Máñez, F. Sancenón, J. Soto and P. Amorós, *Adv. Mater.*, 2007, **19**, 2228–2231.
36 S. Samanta and J. Locklin, *Langmuir*, 2008, **24**, 9558–9565.
37 T. Niazov, B. Shlyahovsky and I. Willner, *J. Am. Chem. Soc.*, 2007, **129**, 6374–6375.
38 L. Baumann, K. Schöller, D. de Courten, D. Marti, M. Frenz, M. Wolf, R. M. Rossi and L. J. Scherer, *RSC Adv.*, 2013, **3**, 23317–23326.
39 L. Dingbin, C. Wenwen, S. Kang, D. Ke, Z. Wei, W. Zhuo and J. Xingyu, *Angew. Chem., Int. Ed.*, 2011, **50**, 4103–4107.